

Analysis of trigonal distortions in $\text{Cs}_2\text{Na}(\text{Al}, \text{Ga})\text{F}_6:\text{Cr}^{3+}$ using experimental EPR data

M. G. BRIK^{a,b}, N. M. AVRAM^{c*}

^a*Fukui Institute for Fundamental Chemistry, Kyoto University, 34-4 Takano Nishihiraki-cho, Sakyo-ku, Kyoto, 606-8103, Japan*

^b*School of Science and Technology, Kwansai Gakuin University, 2-1 Gakuen, Sanda, Hyogo 669-1337, Japan*

^c*Department of Physics, West University of Timisoara, Bd. V. Parvan No. 4, 300223, Timisoara, Romania*

Using the latest experimental data on electron paramagnetic resonance (EPR) measurements for the Cr^{3+} centers in $\text{Cs}_2\text{Na}(\text{Al}, \text{Ga})\text{F}_6$ crystals we derive from the values of the trigonal field parameters, the angles between the C_3 axis and Cr^{3+} -F chemical bonds and relate the signs of the trigonal field parameters to the character of the trigonal deformation. The spin Hamiltonian (SH) parameters (zero-field splitting D , anisotropic g factors g_{\parallel} and g_{\perp}) for trigonal Cr^{3+} centers in $\text{Cs}_2\text{Na}(\text{Al}, \text{Ga})\text{F}_6$ are theoretically investigated by using the perturbation formulas for a $3d^3$ ion in a trigonal symmetry. The calculated SH parameters based on the local geometry are in good agreement with those deduced from the experimental EPR measurements.

(Received October 14, 2005; accepted January 26, 2006)

Keywords: Cr^{3+} center, $\text{Cs}_2\text{Na}(\text{Al}, \text{Ga})\text{F}_6$, trigonal distortion, EPR (ESR) data

1. Introduction

It is well known that when the impurity ion substitutes a host ion in a crystal, the local structure surrounding the impurity becomes different from the corresponding structure in the host crystal. If the impurity is a paramagnetic ion, we can obtain useful information on the local structure of an impurity center by analyzing its EPR data [1, 2, 3], since the EPR parameters of a paramagnetic ion in crystal are sensitive to the local distortion of the impurity center.

Cr^{3+} ion in an octahedral environment is a very attractive system, which is continuously receiving considerable attention of many research groups. By now, about 20 crystals were shown to lase with the Cr^{3+} ion covering the spectral region between 700 nm and 1100 nm [4] and spectroscopic properties of Cr^{3+} ion in many crystals have been reported so far [4,5,6 and references therein].

Very specific energetic structure of Cr^{3+} ion with spin-quartet and spin-doublet levels gives an opportunity to reveal dynamic and static properties of impurity centers formed with this ion [7,8].

Among the crystals doped with trivalent chromium, the fluoride crystals are of a special interest due to their rather low cut-off phonon frequency [9] what causes relatively low non-radiative losses in comparison with oxide crystals [10,11].

Elpasolites which can be schematically represented as A_2BMF_6 (where A, B = Cs^+ , Rb^+ , Tl^+ , K^+ , Na^+ , Li^+ , M = Al^{3+} , Ga^{3+} , V^{3+} , Cr^{3+} , Fe^{3+} , Co^{3+}) represent a large family of isostructural crystals [12].

Recently, comprehensive studies of the hexagonal elpasolites doped with Cr^{3+} were published, including the optical absorption, fluorescence spectroscopy and luminescent quantum efficiency measurements [13, 14, 15, 16], X-ray and neutron diffraction [17, 18], electron paramagnetic resonance (EPR) [19, 20, 21].

According to crystallographic studies [17, 22] in the hexagonal elpasolite lattice there are two inequivalent positions for the trivalent metal. Though the nearest environment is nearly the same for both positions and consists of six fluorines forming an octahedron slightly distorted along the c crystallographical axis, the two positions differ significantly in the next-nearest-neighbor environment. For the first position [12] the $[\text{MF}_6]^{3-}$ octahedron is connected to six $[\text{BF}_6]^{3-}$ octahedra via common corners, and for the second position the $[\text{MF}_6]^{3-}$ octahedron is connected to two $[\text{BF}_6]^{3-}$ octahedra along the c axis through common faces. Thus, this difference should result in different spectroscopic properties of the Cr^{3+} ion, which can occupy them. Indeed, optical [13, 14] and EPR measurements [19, 20, 21] confirmed this conclusion. The spectroscopical parameters (crystal field strength Dq and Racah parameters B and C as well as EPR g -factors and zero field splitting for both equivalent positions have been derived experimentally (they are listed in Tables 1 and 2). EPR technique is very sensitive even to small changes in the structure of an impurity center and, therefore, can be used for an analysis of the distortions in the impurity center. This is the main aim of the present study: using the latest experimental data on EPR measurements for the Cr^{3+} centers in $\text{Cs}_2\text{NaAlF}_6$ and $\text{Cs}_2\text{NaGaF}_6$ crystals [21] we derive from them the values

of the trigonal field parameters for both crystals, calculate the angles between the C_3 axis and Cr³⁺-F chemical bonds and relate the signs of the trigonal field parameters to the character of the trigonal deformation.

Table 1. Spectroscopic parameters for Cs₂NaAlF₆:Cr³⁺ and Cs₂NaGaF₆:Cr³⁺ (in cm⁻¹) [13,14].

| | Cs ₂ NaAlF ₆ | | Cs ₂ NaGaF ₆ | |
|------|------------------------------------|------|------------------------------------|------|
| | I | II | I | II |
| Dq | 1613 | 1600 | 1535 | 1605 |
| B | 740 | 677 | 695 | 730 |
| C | 3308 | 3164 | 3180 | 3295 |

Also we calculate the EPR parameters (zero-field splitting D and g factors $g_{||}$, g_{\perp}) of Cr³⁺ replacing (Al, Ga) in hexagonal elpasolites Cs₂Na(Al, Ga)F₆.

In this paper we investigate theoretically the local trigonal distortion angles of trivalent chromium centers from their EPR spectra by using the perturbation formulas of the spin Hamiltonian parameters for 3d³ ions in trigonally distorted octahedra based on the cluster approach.

2. Calculations of spin – Hamiltonian parameters

Macfarlane [23,24] has considered a d³-ion in a trigonal octahedral center using the high-order perturbation approach. Being based on the strong crystal field scheme, he obtained the following equations for calculating the EPR parameters D , $g_{||}$, $\Delta g = g_{||} - g_{\perp}$ and the first excited state splitting $\delta(^2E)$:

$$D = \frac{2}{9}\xi^2 v \left(\frac{1}{D_1^2} - \frac{1}{D_3^2} \right) - \sqrt{2}\xi^2 v' \left(\frac{2}{3D_1D_4} + \frac{1}{D_2D_3} + \frac{1}{3D_3D_4} \right) + \frac{1}{D_2D_4} + \frac{4\sqrt{2}B}{D_1D_4D_5} + \frac{4B}{D_3D_4D_5} + \frac{9B}{2D_2^2D_3} \quad (1)$$

$$g_{||} = g_s - \frac{8\xi k}{3D_1} - \frac{2\xi^2}{3D_2^2}(k + g_s) + \frac{4\xi^2}{9D_3^2}(k - 2g_s) + \frac{8\xi^2}{9D_1^2}(k - 2g_s) - \frac{4\xi^2 k}{3D_1D_2} + \frac{4\xi^2 k}{9D_1D_3} + \frac{4\xi^2 k}{3D_2D_3} + \frac{8\xi k}{9D_1^2}v - \frac{8\sqrt{2}\xi k}{3D_1D_4}v' \quad (2)$$

$$\Delta g = g_{||} - g_{\perp} = \frac{4\xi k}{3D_1^2}v - \frac{4\sqrt{2}\xi k}{D_1D_4}v' \quad (3)$$

$$\delta(^2E) = E(\bar{E}) - E(2\bar{A}) = 4\xi v \left(-\frac{1}{3D_7} - \frac{4B}{D_7D_{12}} + \frac{B}{D_7D_{13}} - \frac{4B}{D_{10}D_{12}} + \frac{B}{D_{10}D_{13}} \right) + 2\sqrt{2}\xi B v' \left(\frac{4\sqrt{3}}{D_7D_{12}} - \frac{\sqrt{3}}{D_7D_{13}} - \frac{4}{D_8D_{12}} - \frac{1}{D_8D_{13}} \right) \quad (4)$$

In these equations $g_s = 2.0023$, $\xi = k\xi_0$ is the spin-orbit constant in a crystal (reduced with respect to that one ξ_0 for a free ion by the orbital reduction factor $k \approx \left(\sqrt{B/B_0} + \sqrt{C/C_0} \right) / 2$ with B_0 and C_0 being the Racah parameters for a free ion and B and C the Racah parameters in a crystal [25, 26, 27].

The zeroth-order energy denominations D_i are defined in terms of the Racah parameters and crystal field strength Dq as follows:

$$\begin{aligned} D_1 &= \Delta = 10Dq, & D_2 &= 15B + 4C, \\ D_3 &= \Delta + 9B + 3C, & D_4 &= \Delta + 12B, \\ D_5 &= 2\Delta + 3B, & D_7 &= \Delta + 6B, & D_8 &= \Delta + 6B, \\ D_{10} &= \Delta, & D_{12} &= \Delta + 14B + 3C, & D_{13} &= \Delta + 5B. \end{aligned}$$

Finally, the trigonal field parameters v and v' can be expressed using the superposition model of crystal field [28] as

$$v = \frac{18}{7}\bar{A}_2(R)(3\cos^2\theta - 1) + \frac{40}{21}\bar{A}_4(R)(35\cos^4\theta - 30\cos^2\theta + 3) + \frac{40\sqrt{2}}{3}\bar{A}_4(R)\sin^3\theta\cos\theta \quad (5)$$

$$v' = -\frac{6\sqrt{2}}{7}\bar{A}_2(R)(3\cos^2\theta - 1) + \frac{10\sqrt{2}}{21}\bar{A}_4(R)(35\cos^4\theta - 30\cos^2\theta + 3) + \frac{20}{3}\bar{A}_4(R)\sin^3\theta\cos\theta \quad (6)$$

where $\bar{A}_2(R)$ and $\bar{A}_4(R)$ are the intrinsic parameters of the model. For the transition metal ions in octahedral impurity centers $\bar{A}_4(R) = 3Dq/4$ [28,29].

The ratio $\bar{A}_2(R)/\bar{A}_4(R)$ varies from 9 to 12 for many 3d-ions in octahedral environment [26,30,31].

The mean value $\bar{A}_2(R)/\bar{A}_4(R) \approx 10.5$ is often taken [32].

In our calculations we used the value $\bar{A}_2(R)/\bar{A}_4(R) \approx 11.0$, since it provided the best agreement with experimental results. θ is the angle between the C_3 axis and metal-ligand chemical bond. In an ideal octahedron, $\theta = \arccos(1/\sqrt{3}) \approx 54.7^\circ$; in a real (even undoped) crystal this angle differs from that value because of distortions. Precise value of θ can be found, in principle, from the X-ray diffraction data for a given crystal, but, as stated in [33] this value for the doped

crystal should differ from that in the host crystal due to the differences in the mass and ionic radii between the substituted and substituting ions. Using experimental values of the spectroscopic parameters (Table 1), the zeroth-order energy denominations can be readily evaluated. Then, the zeroth-order splitting $2D$ and EPR g -factors can be expressed in terms of θ only. Fig. 1 and 2 show the variations of D and g_{\parallel} , g_{\perp} , when the angle θ changes from 53.7° to 55.7° in $\text{Cs}_2\text{NaAlF}_6:\text{Cr}^{3+}$ (site I). Such interval of θ variation corresponds to small trigonal distortions of the octahedral impurity centers. Behavior of D and g_{\parallel} , g_{\perp} for another site in $\text{Cs}_2\text{NaAlF}_6:\text{Cr}^{3+}$ and both sites in $\text{Cs}_2\text{NaGaF}_6:\text{Cr}^{3+}$ is similar and, therefore, not shown. Analysis of these dependencies shows that the EPR g -factors appear not to depend significantly from the value of θ (they change by less than 1 % only), whereas changing this angle even by few percent can cause a huge variation (even orders of magnitude) in the value of D . That is why the equation for the zero field splitting was chosen for estimate the angle θ .

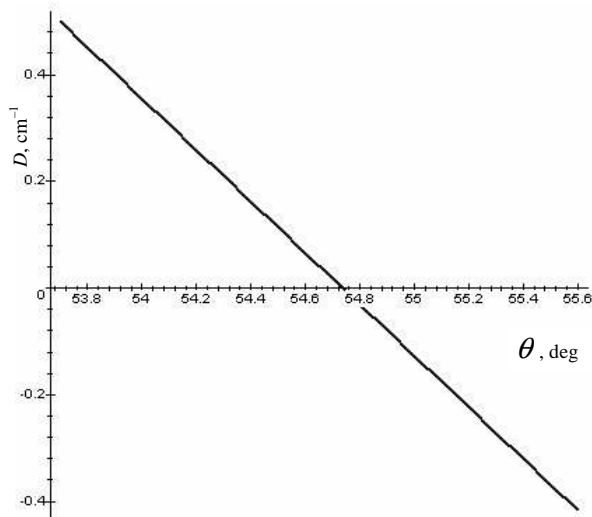


Fig. 1. Dependence of D on the angle between C_3 axis and $\text{Cr}^{3+} - \text{F}$ chemical bond in $\text{Cs}_2\text{NaAlF}_6:\text{Cr}^{3+}$ (site I).

$D = 0$ when $\theta = 54.7^{\circ}$ (no trigonal distortion in this case).

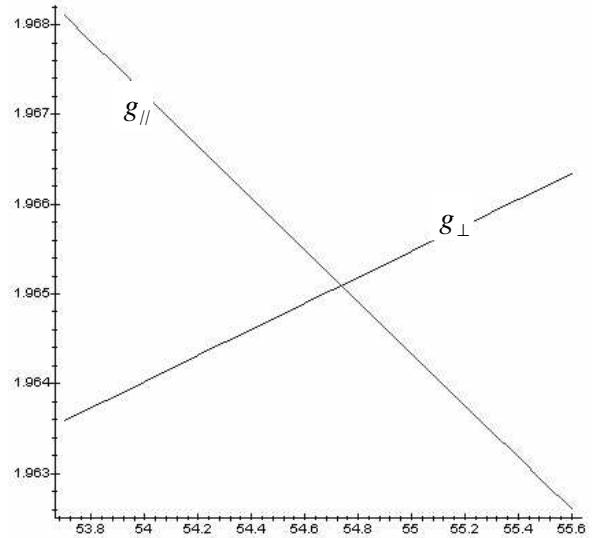


Fig. 2. Dependence of the EPR g_{\parallel} , g_{\perp} factors on the angle between C_3 axis and $\text{Cr}^{3+} - \text{F}$ chemical bond in $\text{Cs}_2\text{NaAlF}_6:\text{Cr}^{3+}$ (site I).

Equating D to the experimental value allows for getting the numerical value of θ , which corresponds to the angle between the C_3 axis and “impurity ion – ligand” chemical bond in the doped crystal. Once this angle is determined, EPR g -factors and trigonal field parameters ν and ν' can be easily evaluated. The results of our calculations are presented in Table 2, in comparison with the experimental data.

3. Discussion

As one can see from Table 2, the results of calculations of the EPR g -factors are in a good agreement with experimental values (the difference between the calculated and measured values is less than 1 %). Since the values of D were used for calculating the value of the angle θ , there is no difference between the calculated and observed values, and the calculated values of D , which are exactly equal to the experimental ones, are not included into the table. Since no experimental data on the first excited state ${}^2\text{E}$ splitting were found in the literature, only the calculated splitting is given. The obtained values of θ are different from those obtained from X-ray analysis [17, 18].

Table 2. Calculation and comparison with experimental results.

| | Cs ₂ NaAlF ₆ | | Cs ₂ NaGaF ₆ | |
|--|------------------------------------|-----------------------|------------------------------------|-----------------------|
| | I | II | I | II |
| k | 0.8962372083 | 0.8668584893 | 0.8736339550 | 0.8923138560 |
| $T = 20$ K | | | | |
| D (cm ⁻¹) [21] | -0.2553 | 0.3911 | -0.2090 | 0.3563 |
| θ , deg (in brackets there are the values obtained by x-ray study [21]) | 55.26592580 (55.0) | 53.91705656 (53.3) | 55.16941108 (55.2) | 53.99725451 (53.2) |
| ν , (cm ⁻¹) | -708.373311 | 1109.856253 | -552.347387 | 1002.880230 |
| ν' , (cm ⁻¹) | 486.103317 | -744.654877 | 378.436444 | -673.798620 |
| $\delta(^2E)$, (cm ⁻¹ , calc) | 13.91 | -21.51 | 11.11 | -19.74 |
| $g_{ }$ (calc.) | 1.9636 | 1.9695 | 1.9638 | 1.9674 |
| g_{\perp} (calc.) | 1.9659 | 1.9660 | 1.9657 | 1.9642 |
| $g_{ }$ (exp.[21]) | 1.9735 ₅ | 1.9730 ₅ | 1.9740 ₅ | 1.9728 ₅ |
| g_{\perp} (exp[21].) | 1.9738 ₅ | 1.9748 ₅ | 1.9736 ₅ | 1.9751 ₅ |
| $T = 300$ K | | | | |
| D (cm ⁻¹) | -0.2590 | 0.3931 | -0.2159 | 0.3626 |
| θ , deg (in brackets there are the values obtained by x-ray study [21]) | 55.27362234 (55.0) | 53.91287641 (53.3) | 55.18374911 (55.2) | 53.98421704 (53.2) |
| ν , (cm ⁻¹) | -718.558969 | 1115.603124 | -570.463143 | 1020.814490 |
| ν' , (cm ⁻¹) | 493.154957 | -748.457403 | 390.940129 | -685.695990 |
| $\delta(^2E)$, (cm ⁻¹ , calc) | 14.11 | -21.62 | 11.47 | -20.09 |
| $g_{ }$ (calc.) | 1.9635 | 1.9695 | 1.9638 | 1.9674 |
| g_{\perp} (calc.) | 1.9659 | 1.9660 | 1.9657 | 1.9641 |
| $g_{ }$ (exp.[21]) | 1.9731 ₅ | 1.9743 ₅ | 1.9722 ₅ | 1.9719 ₅ |
| g_{\perp} (exp[21].) | 1.9737 ₅ | 1.9744 ₅ | 1.9728 ₅ | 1.9747 ₅ |

(experimental error in the last digit are shown by a subscript).

The difference appears to be small, but, nevertheless, it has a crucial importance for getting reasonable agreement between the calculated and experimentally detected values of D , as seen from Fig. 1. Thus, the value of $\theta = 55.0^\circ$ [17, 18] would result in $D = -0.12747$ cm⁻¹, in a poor agreement with experimental value $D = -0.2590$ cm⁻¹.

As seen from data in Table 2, the EPR g -factors, both experimental and calculated, are practically temperature-independent. The dependence of zero field splitting $2D$ on temperature is more essential. Comparison of the obtained values of θ with that of an ideal octahedron suggests the character of the trigonal distortions for both sites. In both crystals, this angle for site I is greater than 54.7° , and the deformation in this case is compression along the C_3 axis. The value of θ for

site II in both crystals is smaller than 54.7° , and the deformation is elongation along the C_3 axis. The signs of D and trigonal field parameters are opposite for both sites. The absolute values of ν and ν' for site II are greater than those for site I, therefore the low-symmetry component of crystal field at site II is more pronounced than for site I. The values of the trigonal field parameters defined in this paper from the experimental EPR results are believed to be more precise and reliable than those estimated from the optical absorption spectra [34,35].

4. Conclusions

The main purpose of this paper is to study theoretically the local trigonal distortion angles of Cr³⁺

centers in hexagonal elpasolite fluorides $\text{Cs}_2\text{Na}(\text{Al}, \text{Ga})\text{F}_6$ from their EPR spectra by using the perturbation formulas of the spin Hamiltonian parameters in trigonally distorted octahedra based on the cluster approach.

The comparison between the obtained result and experimental data has been carried out. The different sign of zero field splitting energy is explained by different values of distortion angles around the impurity ions.

Acknowledgments

M.G. Brik acknowledgement of the financial support from the Japanese Ministry of Education, Culture, Sports, Science and Technology (MEXT) in a project on Computational Materials Science unit at Kyoto University.

References

- [1] W.- C. Zheng, *J. Phys. Chem. Solids* **56**, 61 (1995).
- [2] W.- C. Zheng, *Physica* **B245**, 119 (1998).
- [3] V. - K. Jain, *Z. Naturforsch.* **58a**, 667 (2003).
- [4] S. Kück, *Appl. Phys. B* **72**, 515 (2001).
- [5] M. Grinberg, *Opt. Mater.* **19**, 37 (2002).
- [6] P. A. Tanner, *Chem. Phys. Lett.* **388**, 488 (2004).
- [7] A. N. Medina, A. C. Bento, M. L. Baesso, F. G. Gandra, T. Catunda, A. Cassanho, *J. Phys.: Condens. Matter* **13**, 8435 (2001).
- [8] O. S. Wenger, R. Valiente, H. U. Gudel, *J. Chem. Phys.* **115**, 3819 (2002).
- [9] B. Henderson, R. H. Bartram, *Crystal-Field Engineering of Solid-State Laser Materials*, Cambridge University Press, Cambridge, (2000);
- [10] S. A. Payne, L. L. Chase, H. W. Newkirk, L. K. Smith, W. F. Krupke, *IEEE J. Quant. Electron.* **24** 2243 (1988).
- [11] M. G. Brik, C. N. Avram, *J. Lumin.* **102-103**, 283 (2003).
- [12] D. Babel, R. Haegele, G. Pausewang, F. Wall, *Mater. Res. Bull.* **8**, 1371 (1973).
- [13] L. P. Sosman, A. Dias Tavares Jr., R. J. M. da Fonseca, T. Abritta, N. M. Khaidukov, *Solid State Commun.* **114**, 661 (2000).
- [14] R. J. M. da Fonseca, A. Dias Tavares Jr., P. S. Silva, T. Abritta, N. M. Khaidukov, *Solid State Commun.* **110**, 519 (1999).
- [15] R. J. M. da Fonseca, L. P. Sosman, A. Dias Tavares Jr., H. N. Bordallo, *J. Fluoresc.* **10**, 375 (2000).
- [16] G. A. Torchia, D. Schinca, N. M. Khaidukov, J. O. Tocho, *Opt. Mater.* **20**, 301 (2002).
- [17] H. N. Bordallo, R. W. Henning, L. P. Sosman, R. J. M. da Fonseca, A. Dias Tavares Jr., K. M. Hanif, G. F. Strouse, *J. Chem. Phys.* **115**, 4300 (2001).
- [18] H. N. Bordallo, X. Wang, K. M. Hanif, G. F. Strouse, R. J. M. da Fonseca, L. P. Sosman, A. Dias Tavares Jr., *J. Phys.: Condens. Matter* **14**, 12383 (2002).
- [19] E. Fargin, B. Lestienne, J. M. Dance, *Solid State Commun.* **75**, 769 (1990).
- [20] H. Vrielinck, N. M. Khaidukov, F. Callens, P. Matthys, *Radiat. Eff. Defects Solids* **157**, 1155 (2002).
- [21] H. Vrielinck, F. Loncke, F. Callens, P. Matthys, N. M. Khaidukov, *Phys. Rev. B* **70**, 144111 (2004).
- [22] N. I. Golovastikov, N. V. Belov, *Kristallografiya* **23**, 42 (1978).
- [23] R. M. Macfarlane, *J. Chem. Phys.* **47** 2066 (1967).
- [24] R. M. Macfarlane, *Phys. Rev. B* **1** 989 (1970).
- [25] M. G. Zhao, J. A. Xu, G.R. Bai, H.S. Xie, *Phys. Rev. B* **27**, 1516 (1983).
- [26] W. C. Zheng, S. T. Wu, *J. Phys.: Condens. Matter* **11**, 3127 (1999).
- [27] Z. Y. Yang, C. Rudowicz, J. Qin, *Physica B* **318**, 188 (2002).
- [28] D. J. Newman, B. Ng, *Rep. Progr. Phys.* **52**, 699 (1989).
- [29] W. L. Yu, M. G. Zhao, *Phys. rev. B* **37**, 9254 (1988).
- [30] W. C. Zheng, S. Y. Wu, *Mater. Sci. Eng. B* **97**, 235 (2003).
- [31] A. Edgar, *J. Phys. C* **9** 4303 (1976).
- [32] W.-C. Zheng, Q. Zhou, Y. Mei, X.-X. Wu, *Opt. Mater.* **27**, 449 (2004).
- [33] C. Rudowicz, Z.-Y. Yang, Y.-Y. Yeung, J. Qin, *J. Phys. Chem. Solids* **64**, 1419 (2003).
- [34] R. M. Macfarlane, *J. Chem. Phys.* **39**, 3118 (1963).
- [35] M. G. Brik, N. M. Avram, C. N. Avram, *Solid State Commun.* **132**, 831 (2004).

Invited Lecture

*Corresponding author: avram@physics.uvt.ro